STRUCTURAL STUDIES OF BACTERIOPHAGE T7 AND T7 CAPSIDS

Thesis by

John Edward Ruark

In Partial Fulfillment of the Requirements for the Degree of

Master of Science

California Institute of Technology
Pasadena, California 91125

1978

(Submitted July 1, 1977)

I. Acknowledgements

I would like to thank Dr. Robert M. Stroud for his support during my time at the California Institute of Technology. Further, it is my pleasure to acknowledge the collaboration, insight, and friendship of Dr. Michael Jay Ross throughout the work described herein.

II. Abstract

The structures of bacteriophage T7 and T7 capsids have been investigated by small-angle X-ray scattering. Phage T7 has a radius of 301 ± 2 Å (excluding the phage tail), and a calculated volume of $1.14 \pm .05 \times 10^{-16}$ ml. The radius determined for T7 phage in solution is about 30% greater than the radius measured from electron micrographs, indicating that considerable shrinkage and distortion occurs during sample preparation for electron microscopy. Thus the volume calculated from X-ray scattering in solution is almost twice that estimated from electron microscope measurements. Capsids that have a phage-like envelope and do not contain DNA were obtained from lysates of T7-infected E. coli (capsid II) and by separating the capsid component of T7 phage from the phage DNA using temperature shock (capsid IV). These capsids have outer radii of 2^3-289 ± 2 Å and are thus significantly smaller than the envelope of T7 phage. The thickness of the envelopes of two forms of capsid II are 20 and 23 ± 2 Å. The volume in T7 phage available to package DNA is estimated to be $9.2 \pm .4 \times 10^{-17}$ ml or 2.1 times the volume of the B form of T7 DNA.

A T7 precursor capsid (capsid I), believed to be capable of pulling in DNA, has a smaller outer diameter (261 ± 2 Å) and a thicker envelope (52 ± 4 Å) than capsids II and IV. Capsid I expands when pelleted in the ultracentrifuge, but expansion can be prevented by fixing with glutaraldehyde. A low resolution model for the capsid I envelope has been developed.

TABLE OF CONTENTS

IV. Dedication

For Martha Ann Morrison
In memory of the sweetness and sadness of a youthful dream.

V. Introduction

The phenomenon of viral self-assembly, as well as the nature of the structures which result from such a process, are questions currently evoking considerable interest. This becomes particularly apparent when one recalls the growing body of evidence linking viruses or viral genetic material with a number of human maladies, most notably cancer (1-5). It is motivated by such concerns that it has been undertaken to employ x-ray diffraction techniques in an investigation of viral structures related to the self-assembly sequence of the bacteriophage T7.

T7 phage is a strictly virulent coliphage, and is the smallest of the seven original T phages discovered concurrently by Delbrück, and Demerec and Fano in 1945. It consists of a polyhedral head with a small cylindrical tail (see Figures 7, 8, Appendix A), and estimates from electron microscopy place the diameter of the head of native (or infectious) T7 phage between 540 and 575 Å (6), while the size of the tail has been similarly gauged at roughly 100 by 150 Å. T7 also possesses an internal protein moiety termed a core, which appears to be a cylindrical structure about 200 Å in length and roughly 150 Å in diameter, with a hole down the center, and which may be seen in Figure 1 as well. The total mass of native T7 phage is about 49 million daltons, 25 million of which comprise the double-stranded linear DNA molecule which constitutes the genome of this particle (7). Prior to the assembly of the completed phage, this DNA molecule has been shown to exist in a concatameric precursor composed of up to ten full genetic complements (8), and evidence exists that each single

complement is chopped loose from the precursor directly following incorporation into the assembled phage head.

SDS polyacrylamide gel electrophoresis has revealed about 30 protecins associated with T7, with molecular weights ranging from 7,000 to 150,000 daltons (7), and these appear to account for virtually all of the coding capacity of the genetic material (7). Studies employing conditionally lethal amber mutants as well as a number of deletion mutants have revealed nineteen essential genes specified in the T7 genome (7). The phage head in particular has been found to contain proteins corresponding to gene 8 (62,000 daltons), gene 9 (40,000 daltons), gene 10 (38,000 daltons), gene 14 (18,000 daltons), gene 15 (83,000 daltons), and gene 16 (150,000 daltons), with the gene 10 protein (dubbed the major head protein) accounting for 60% of the mass (excluding DNA) of the mature phage head (9).

There are a number of T7 phage-related structures which are relevant to the self-assembly sequence of the phage, and a schematization of these structures as well as the relationships between them may be seen in Figure 1. The diagrams shown in this figure of the various heads are based on electron micrographs of the isolated structures, and examples of such micrographs may be seen as well in Appendix A.

The protein which is coded by gene 9 of the T7 genome is of particular interest because of its apparently crucial role in the maturation of infective T7 phage. It is termed the DNA incorporation protein, and is found in significant quantity only in heads which do not contain DNA (9). Conversely, mutants which are defective in this gene fail to incorporate DNA or to form heads, and all indications are

that the gene 9 protein is ejected either during or closely preceding the actual DNA incorporation (9). Structures may be isolated which are equivalent to those which result from a mutation in the phage's DNA polymerase gene (which thus make no DNA to incorporate) that contain the gene 9 protein in roughly a third the quantity of the major head protein (as well as a core and no tail), and these mutant-like heads have been dubbed Capsid I. Capsid I seems to be a relatively fragile structure, and on sedimentation appears in the electron microscope to assume a "relaxed" conformation, which we designate Capsid Ia. However, if Capsid I is "fixed" by exposure to a 3% solution of glutaraldehyde, it appears in the electron microscope to retain a structure which is similar to the unfixed Capsid I even after high speed sedimentation. Glutaraldehyde-fixed Capsid I is herein designated Capside Ib.

A second structure which results from wild-type T7 phage infections is a head which apparently ejects the DNA incorporation protein while failing to incorporate DNA. This structure, consisting of a shell of major head protein and a core assembly, is herein denoted Capsid II. In the electron microscope, Capsid II appears larger than Capsid I, and its shell seems thinner. However, one of the primary motivations for undertaking this study in solution lies in the artifactual nature of electron micrographs due to the rigorous nature of the sample preparation required. In particular, two effects may be anticipated. The first of these is shrinkage of the phage particles due to the dehydration which is a necessary concomitant of the sample preparation. The second is flattening of the structures on the grids

due to simple gravitational distortion once they are out of solution. This flattening effect, which would make a structure appear larger in a micrograph than it is in solution, has been estimated employing a tilting stage electron microscope at about 3:1 for native T7 phage (6) and one might anticipate an even greater effect for empty-headed structures such as Capsid II. Thus, these two artifacts should tend to balance each other to varying unknown degrees in the electron microscope, and a determination of the structures of viral particles in solution becomes imperative in assessing their true dimensions.

It is possible by various manipulations of the infectious phage particles to generate heads which are closely related to the naturally-occurring mutants. As depicted in Figure 1, if the phage are warmed to 50°C for 35 minutes, they expel their DNA and cores while retaining their tails to form heat-shocked heads, which are also termed Capsid IVb. Alternatively, if the native T7 particles are exposed to 1% SDS in addition to the above warming, they lose their tails as well as their DNA and c ores to form simple shells which are designated SDS heads, or Capsid IVa.

Each of the above structures has been subjected to low-angle x-ray diffraction in an attempt to determine its radial electron density, from which it may prove possible to reach some conclusions about the nature of the mature virus, as well as the self-assembly process which produced it.

A number of investigators have undertaken previously to examine the low-angle x-ray diffraction of virus particles in solution in order to determine some aspect of their structures (10-12). In

general, the most detailed information which has been accessible by this technique is spherically-averaged radial electron density distribution, which is of particular interest if the particle under consideration possesses roughly spherical symmetry itself. This relative one-dimensional electron density is accessible through a Fourier inversion of a similarly one-dimensional trace of the observed scattering from icosahedral viruses in solution, this diffraction generally consists of a series of regularly spaced concentric circular maxima the profile of which resembles a $\frac{\sin x}{x}$ curve. The positions and intensities of these maxima are functions of the radii and radial electron densities of the particles under consideration (13).

If one assumes spherical symmetry, then the scattering from a single particle is proportional to the square of the structure factor F(h), which may be defined in this case as follows (13):

$$F(h) = \int_0^\infty \rho(r) \frac{\sin hr}{hr} 4\pi r^2 \, dr \qquad (1)$$

where $h = 4\pi \sin\theta/\lambda$, 2θ being the angle at which the intensity is measured, and λ being the wavelength of the probing radiation. In addition, $\rho(r)$ is here taken to be the average radial electron density at distance r from the center of the particle. This formulation has been shown for a uniformly dense sphere of radius R to yield a diffraction pattern defined by the following expression (14):

$$F(h) = \frac{4\pi}{h^3R^3} [\sin hR - hR \cos hR] \qquad (2)$$

In the case of spherical shells, the following formalism may be derived. $\rho(r)$ is assumed equal to zero except between r_1 and r_2, where it is assumed equal to one. Equation (1) reduces to:

$$F(h) = \frac{4\pi}{h} \int_{r_1}^{r_2} r \sin hr \, dr \tag{3}$$

This integral is a standard form whose solution may be written as follows:

$$F(h) = \frac{4\pi}{h} \left[\frac{1}{h^2} \sinh r - \frac{r}{h} \cosh r\right]_{r_1}^{r_2}$$

$$= \frac{4\pi}{h} \left[\frac{1}{h^2} \{\sin hr_2 - \sin hr_1\} - \frac{r_1}{h}\{\cos hr_2 - \cos hr_1\} - \frac{r_2 - r_1}{h}\{\cos hr_2\}\right]. \tag{4}$$

Application of standard trigonometric identities yields the following expression:

$$F(h) = \frac{4\pi}{h^3} \sin \frac{h(r_2 - r_1)}{2} \left\{\cos \frac{h(r_2 + r_1)}{2} + hr_1 \sin \frac{h(r_2 + r_1)}{2}\right\}$$

$$- \frac{4\pi(r_2 - r_1)}{h^2} \cos hr_2. \tag{5}$$

If we define the shell center $r_3 = \frac{r_2 + r_1}{2}$ and the shell thickness $t = r_2 - r_1$, we have

$$F(h) = \frac{4\pi}{h^3} \sin\frac{ht}{2} \{\cos hr_3 + h(r_3+\frac{t}{2}) \sin hr_3\} - \frac{4\pi t}{h^2} \cos(r_3+\frac{t}{2}). \quad (6)$$

Finally, further application of standard trigonometric identities and algebraic manipulations results in the following expression:

$$F(h) = \frac{4\pi}{h^3} [hr_3 \sin\frac{ht}{2} \sin hr_3 + \cos hr_3 \sin\frac{ht}{2} - \frac{ht}{2} \cos hr_3 \cos\frac{ht}{2}]. \quad (7)$$

This fairly complex expression indicates a number of high frequency terms dependent on the shell center position modulated by lower frequency terms dependent on the shell thickness. Hence, node positions are expected to be primarily sensitive to the shell center, while relative intensities of maxima should be primarily sensitive to the shell thickness. These expectations are borne out in computer experiments with perfect shells (see Appendix A).

It has been demonstrated (13) that positions and relative amplitudes of diffraction maxima should not change as the system under examination is expanded from a single diffracting particle to a number of particles in solution, as long as concentrations are maintained at a low enough level that interparticle interference remains negligible. Thus, the scattering from a randomly oriented noninterfering solution of particles will be directly proportional to the scattering from a single particle, rendering equations (1) and (2) directly applicable to low-angle diffraction in solution.

As with most diffraction techniques, in this case the knowledge of the position and the amplitude of an intensity is insufficient to

permit complete analysis in itself. The additional factor which must be surmised is the phase of a given intensity with respect to the phase of the probing beam. In a one-dimensional system such as the one under consideration this problem of phase assignment reduces to one of designating the value of the structure factor (proportional to the square root of the observed intensity) as either positive or negative with respect to the incident beam. The problem of the determination of these phases is examined in Appendix A.

Figure 1

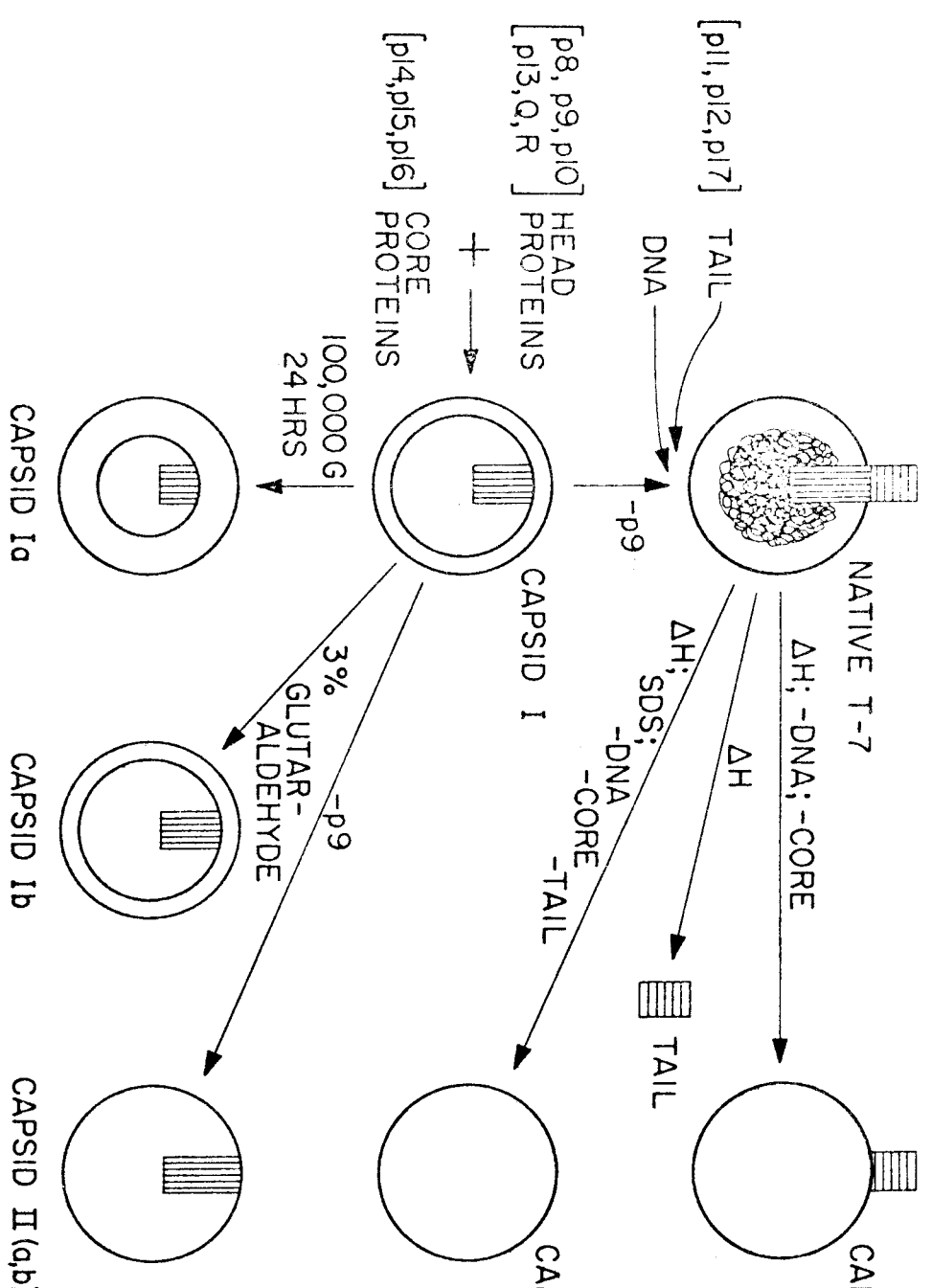
[pII, pI2, pI7] TAIL
DNA
[p8, p9, pI0 pI3, Q, R] HEAD PROTEINS
+
[pI4, pI5, pI6] CORE PROTEINS
100,000 G 24 HRS
-p9
NATIVE T-7
CAPSID I
CAPSID Ia
CAPSID Ib
CAPSID II (a,b)
3% GLUTAR-ALDEHYDE
-p9
ΔH; SDS; -DNA -CORE -TAIL
ΔH
ΔH; -DNA; -CORE
TAIL
CAPSID IVa
CAPSID IVb

REFERENCES

1. W. Rawls, M. Castron, and P. Rapp (1974), Cancer Res. 34, 362-366.
2. P. Rozinan and P. Frankel (1973), Cancer Res. 33, 1402-1416.
3. L. Henle and W. Henle (1973), Cancer Res. 33, 1419-1423.
4. R. McAllister and M. Nicolson (1972), Nature New Biol. 235, 3-6.
5. S. Spiegelman, L. Kufe, J. Hehlman, and J. Peters (1973), Cancer Res. 33, 1515-1526.
6. P. Serwer (1977)--submitted to J. Ultrastruc. Res.
7. F.W. Studier (1972), Science 176, 367-376.
8. P. Serwer (1974), Virology 59, 89-107.
9. P. Serwer (1976), J. Mol. Biol. 107, 271-292.
10. R. Fischbach and S. Harrison (1965), J. Mol. Biol. 13, 638-645.
11. S. Harrison (1969), J. Mol. Biol. 42, 457-483.
12. W. Earnshaw, S. Casjens, and S. Harrison (1976), J. Mol. Biol. 104, 387-410.
13. A. Guinier and G. Fournet, Small Angle Scattering of X-Rays, Chapters 2 and 4. Wiley, New York, 1955.
14. L. Rayleigh (1914), Phil. Mag. 6, 321.

VI. Appendices

Appendix A : Paper : Structural Study of Bacteriophage T7 and T7 Capsids

Structural Study of Bacteriophage T7 and T7 Capsids

JOHN E. RUARK*, PHILIP SERWER†, MICHAEL J. ROSS‡ AND ROBERT M. STROUD§

Norman W. Church Laboratory of Chemical Biology

California Institute of Technology

Pasadena, California 91125, U.S.A.

(Received _____)

RUNNING TITLE: Structural study of phage T7

*Present Address: School of Medicine, Stanford University, Stanford Ca. 94305

†Present Address: Department of Biochemistry, Houlter Sciences Center, University of Texas, 79287

‡Present Address: Biological Laboratories, Harvard University, Cambridge, Mass. 02738.

§Present Address: Dept. of Biophysics & Biochemistry, School of Medicine, U.C. San Francisco 94143.

Abstract

The structures of bacteriophage T7 and T7 capsids have been investigated by small-angle X-ray scattering. Phage T7 has a radius of 301 ± 2 Å (excluding the phage tail), and a calculated volume of $1.14 \pm .05 \times 10^{-16}$ ml. The radius determined for T7 phage in solution is about 30% greater than the radius measured from electron micrographs, indicating that considerable shrinkage and distortion occurs during sample preparation for electron microscopy. Thus the volume calculated from X-ray scattering in solution is almost twice that estimated from electron microscope measurements. Capsids that have a phage-like envelope and do not contain DNA were obtained from lysates of T7-infected E. coli (capsid II) and by separating the capsid component of T7 phage from the phage DNA using temperature shock (capsid IV). These capsids have outer radii of 283-289 ± 2 Å and are thus significantly smaller than the envelope of T7 phage. The thickness of the envelopes of two forms of capsid II are 20 and 23 ± 2 Å. The volume in T7 phage available to package DNA is estimated to be $9.2 \pm .4 \times 10^{-17}$ ml or 2.1 times the volume of the B form of T7 DNA.

A T7 precursor capsid (capsid I), believed to be capable of pulling in DNA, has a smaller outer diameter (261 ± 2 Å) and a thicker envelope (52 ± 4 Å) than capsids II and IV. Capsid I expands when pelleted in the ultracentrifuge, but expansion can be prevented by fixing with glutaraldehyde. A low resolution model for the capsid I envelope has been developed.

2. Introduction

Icosahedral DNA bacteriophages have a shell of protein subunits arranged to form a polyhedron which encloses the genetic material. The bacteriophages also contain a tubular tail assembly and tail fibers for attachment to the host bacteria. The length of the DNA is 300-500 times the diameter of the head (Tikchonenko, 1969) and must be packaged within the head volume during the morphogenesis of the bacteriophage. Phage T7 is an excellent candidate for structural study of DNA packaging, since it has a smaller genome than most double strand DNA phages, and it is probable that the full complement of 30 proteins coded for by this genome have been identified (Studier & Maizel, 1969; Studier, 1972). Since T7 is a nonpermutative phage it may be possible to alter the electron density due to DNA inside the phage head. The prohead of T7 has been isolated and characterized, and in addition, several other empty shell structures and packaging mutants have been isolated. In this paper we report studies of several of these structures. We correlate the results with the chemical and physical alterations which accompany the process of DNA packaging in T7.

Current evidence indicates that DNA is packaged in the head of phage T7 and some other DNA bacteriophages when an assembled precursor capsid draws in DNA, presumably through a hole in the capsid envelope (reviewed in Casjens & King, 1975). In the case of phage T7, the precursor capsid (capsid I)[1] and the intact phage have been examined by electron microscopy (Serwer, 1976) and found to contain an internal cylindrical core. The core contains an axial hole which is contiguous

with a hole in the capsid envelope. In the electron microscope, the shell of capsid I appears smaller in diameter and thicker than the shell of T7 phage. A major protein component of capsid I, $p\text{-}9^2$, is lost during the packaging process (Serwer, 1976) and is found in the assembled phage in comparatively small amounts. Thus, there appear to be major structural changes in the capsid during DNA packaging.

Although T7 capsids and phage have been observed in the electron microscope, there are indications that the dimensions of these structures as measured by electron microscopy are subject to large systematic errors. There is a strong possibility that shrinkage may occur during drying for electron microscopy because the capsids do not contain DNA and the DNA in T7 phage is highly hydrated (Serwer, 1975). The inherent inaccuracy of electron microscope measurements is compounded by the tendency of T7 phage and its capsids to flatten on the electron microscope grid during negative staining (Serwer, 1977). Using the published values for negatively stained phage of 550 $\mathring{A}$ for the diameter of the particle (North and Rich, 1961; Serwer, 1977) and of 35 $\mathring{A}$ for the thickness of the protein shell (Bradley, 1965), the volume of the interior of the phage head is 5.8×10^{-17} ml. North & Rich (1961) have attributed the 24 $\mathring{A}$ X-ray diffraction reflection from T7 phage to the interhelix distance of the DNA when packaged. The volume occupied by the T7 genome in a hexagonal lattice with this spacing (which would define the minimum possible space occupied by the packaged DNA) would be 8.7×10^{-17} ml, over 50% larger than the interior volume of the head. Further, studies of the buoyant density of T7 in sodium iothalamate

indicate that the volume of the B-form of T7 DNA is about half the total phage volume (Serwer, 1975), or about 72% of the interior volume of the shell. These discrepancies may be most readily accounted for by the artifactual nature of electron microscopy.

Accurate measurements of the dimensions of T7 phage and capsids can be made on the various species in solution using X-ray diffraction. Both T7 and its capsids appear in the electron microscope to have a relatively high degree of spherical symmetry (Serwer, 1976), allowing their Fourier transforms to be described by a series of terms, the first set of which is independent of angular coordinates (Harrison, 1969). These terms are related to spherical Bessel functions, and will dominate the X-ray diffraction pattern to the resolution that the irradiated particles are spherically symmetric. The diffraction arising from these terms allows for determination of the average electron density of particles as a function of distance from the center of the particle (Guinier & Fournet, 1954; Finch & Holmes, 1967).

In the present communication we report determinations of the radial electron density distributions of phage T7 and T7 capsids. The implications of the results for understanding DNA packaging in T7 and for the interpretation of electron micrographs are discussed.

3. Materials and Methods

a. Phage and bacterial strains

Wild-type bacteriophage T7 and T7 amber mutant 28 (DNA polymerase) (Studier, 1969) were obtained from F. W. Studier. *E. coli* BB/1 was the host for wild-type T7 and was the nonpermissive host for the amber mutant. *E. coli* 0-11' was the permissive host for the amber mutant.

b. Media and buffers

Stocks of wild-type T7 phage were grown in M9 medium at 30° C (Kellenberger and Sechaud, 1957). Stocks of the amber mutant were grown in T broth (10 gm tryptone, 5 gm NaCl, 10ℓ water) at 30° C. Buffers used were: 1) Tris/Mg buffer: .2 M NaCl, .01 M Tris, pH 7.4, .001 M $MgCl_2$. 2) Phos/Mg buffer: .2 M NaCl, .01 M sodium phosphate, pH 7.2, .001 M $MgCl_2$.

c. Preparation of T7 phage and capsids

Lysates were prepared as follows: An overnight culture of *E. coli* BB/1 in M9 + 2% T broth was diluted 1:100 into 15 liters of M9 medium. The culture was grown with aeration to 3-4 x 10^8 bacteria/ml, and was then infected with phage. For wild-type phage the multiplicity of infection was .05 - .1 and for mutants the multiplicity was 10. High titer stocks of mutant phage were prepared by polyethylene glycol (Carbowax 6000, Union Carbide) precipitation (see below) from permissive lysates.

Phage T7 and T7 capsids were precipitated from the lysates using polyethylene glycol and were purified on a combination of cesium

chloride step and buoyant density gradients as described in Serwer (1976), except that cell debris was removed by centrifugation at 10,000 rpm for 20 min in a Sorvall GSA rotor (the slower speed used in previous studies does not remove as much debris). The capsids were further purified by sedimentation through 5-25% sucros gradients. When 1-10 mg of capsid I were sedimented, the capsid I peak was generally skewed to the faster sedimenting side. The amount of skewing depended on the amount of material on the gradient, and the contents of fractions collected from various regions in the skewed peak were indistinguishable in the electron microscope. Thus, the skewing probably resulted from a reversible aggregation of capsid I particles.

Capsid II was resolved into two bands on the sucrose gradient differing by 7% in sedimentation rate. The material in the slower band will be referred to as capsid IIa and capsids in the faster band as capsid IIb (Serwer, 1976).

T7 phage were dialyzed against Tris/Mg buffer. Capsids were either dialyzed against Tris/Mg buffer or were stored in sucrose without dialysis, as indicated in the figure legends or text.

d. Electron microscopy

Fenestrated grids with their holes covered by a light carbon film were prepared as in Serwer (1976). Electron micrographs were made of particles over holes in the fenestrated film where contrast was optimal. Specimens were observed with a Phillips 301 electron microscope.

T7 phage were prepared for electron microscopy as follows: 3-5 µl of phage solution were placed on an electron microscope grid

for 1 min. The grid was washed with 4 drops of distilled water and then 2 drops of 1% uranyl acetate. The grid was dried with filter paper. In the case of capsid structures, 3-5 µl of capsid solution in Tris Mg buffer were placed on an electron microscope grid for 1 min. The excess solution was removed by touching the droplet with a Pasteur pipet. Before the liquid film dried a drop of 1% sodium phosphotungstate pH 7.6 was placed on the grid. The grid was then dried with filter paper.

Capsid samples for demonstrating pelleting-induced alteration were prepared for electron microscopy in the following manner: A 3 µl sample of capsid I from a wild-type lysate was taken without dialysis from a sucrose gradient. The sample was fixed by mixing with 1 µl of 12.5% glutaraldehyde in 0.5 M sodium phosphate, pH 7.2. The fixed sample was layered on 5.2 ml of Phos/Mg buffer in a nitrocellulose centrifuge tube for a Beckman SW50.1 rotor (the sample sank to the bottom). This fixed sample and an unfixed sample of the same material was pelleted (30k, 16 hr, 4°C) and was resuspended in 20 µl of Phos/Mg buffer. A similar unfixed sample of capsid I from polymerase minus mutants was also pelleted in similar fashion. The fixed sample and the unfixed mutant capsids were prepared for electron microscopy as follows: A 3-5 µl droplet of sample was placed on an electron microscope grid for 1 min. The grid was washed with four drops of water and then two drops of 1% sodium phosphotungstate, pH 7.6. The grid was dried with filter paper. The unfixed, wild-type capsids were prepared for electron microscopy in the same fashion as described for capsids above.

e. Sample preparation for X-ray diffraction

The concentration of samples used for X-ray diffraction were between 5 mg/ml and 500 mg/ml. Unfixed samples were suspended in Tris/Mg buffer; samples fixed in glutaraldehyde were suspended in Phos/Mg buffer (glutaraldehyde reacts with Tris buffer and induces a lowering of the pH). Concentrations of capsids were determined by the method of Lowry et al. (1951); phage T7 concentrations were estimated by UV absorbance ($E^{1\%}_{260} = 9.78 \times 10^3$ (Bancroft & Freifelder, 1970)). To obtain the high concentrations needed for diffraction, samples were concentrated by sedimentation at 100,000 G for 24 hours, after which the supernatant was withdrawn to a known volume, and the resulting pellet was allowed to resuspend for 24 hours. Phage and capsids subjected to this treatment were examined by centrifugation and electron microscopy. Negligible denaturation was found after this pelleting procedure with one exception (see below).

Solutions for X-ray investigation were contained in 0.7 mm thin-walled glass capillaries sealed with dental wax, or between the flat cellulose acetate windows of a plexiglass sample holder. Sample temperature was maintained between 1 and 5° C throughout. Electron microscopy of T7 capsids and phage was conducted concurrently with diffraction experiments.

f. X-ray data collection

X-ray scattering was recorded on Kodak "no-screen" X-ray film. The X-ray source was an Elliot GX6 rotating anode generator operating at 500 to 1000 watts with a 100-micron focus. Nickel-filtered Cu Kα radiation was doubly focused using elliptically-bent fused silica flats

which were mounted so as to focus in both the horizontal and vertical planes (Ross & Stroud, manuscript in preparation). The incident beam was always focused onto the film plane, and the focused beam cross section (width at half height) measured from a short exposure of the direct beam was about 300 microns.[3]

The low-angle camera incorporated guard slits to minimize parasitic scatter and to isolate the doubly-reflected beam from the straight-through and singly-reflected beams. The sample was maintained at 4° C, and the specimen to film space consisted of a helium-filled chamber which included the film cassette. The direct beam passed through a 1-mm hole in the film center and the beam stop was behind the film. About five exposures, ranging in time from one to 120 hours, were used to record the entire small-angle diffraction for each structure examined. Short-term exposures used to record low-order scattering were made from more dilute solutions (< 10 mg/ml) in order to avoid complexities due to interparticle interference. Multiple film packs were not used when analyzing data extremely close to the direct beam, since we have observed parasitic scattering in this region (corresponding to $1/s > 400$ Å) which was traced to the presence of multiple films. The diffraction pattern recorded for capsid II is shown in Figure 2.

g. Data processing

Small-angle films were converted into digitized arrays of optical densities on a Syntex Analytical AD-1 flatbed, moving stage, automicrodensitometer (Ross & Stroud, 1977). Scanner spot size and

raster were both 32 microns square.

Diffraction rings on the film were radially integrated and displayed as the average value of h(s) versus s. Regions of the film containing residual parasitic scatter from the focusing mirrors and guard slits were left out of the integration. In order to correctly integrate the pattern, it was necessary to accurately determine the diffraction center. This was done by iterative refinement of the film center position, with respect to peak maxima in each quadrant of the film. (Approximate film centers, determined from short exposures of the direct beam, were in error by as much as 120μ. This factor is significant, since a centering error of 30μ introduces considerable artificial smearing of the data on radial integrations.) Refined centers were generally determined to within ±10μ.

An iterative method was chosen to deconvolute the beam profile from the diffraction pattern (Mencik, 1974). (See Figure 3.) In order to implement the deconvolution, the beam profile g(s) was numerically convoluted with the observed data h(s) to produce a doubly convoluted profile h'(s). The difference between h'(s) and h(s) was taken as a first approximation of the error introduced by the experimental convolution, and was subtracted from h(s) to give a first-order corrected profile f'(s). The f'(s) was convoluted with the beam profile and compared with h(s) to obtain a second-order correction. The process was iterated until no improvement in f'(s) occurred. The extent of convergence is defined as

$$\Delta = \frac{\int_{S=0}^{S} |h'(s) - h(s)|\, ds}{\int_{S=0}^{S} |h(s)|\, ds} .$$

The value of Δ was typically 4% at convergence. The extent of artificial diminution of peak heights that would result if this process were not applied can readily be seen in Figure 3.

Multiple exposures were scaled together to give the complete small-angle scattering pattern from $1/s_{min} \simeq 600$ Å to $1/s_{max} \simeq 35$ Å. The central region of the pattern, unobservable because of interference by the direct beam noise, was determined by extrapolation as follows. Native T7 phage is roughly spherical in the electron microscope (see below) and its hydrated DNA component has roughly the same mass density (and therefore electron density) as its hydrated protein (Serwer, 1975). The inner two-thirds of the central maximum was thus estimated from a Guinier plot [ln h versus $\sin^2\theta$ (Guinier & Fournet, 1955)]. The capsids appear as approximated spherical shells in the electron micrographs (see Figure 2) and linear Guinier plots would not result from the intensity profile of such structures. The unobserved portion of the central maximum of the diffraction pattern from each of these capsids was left out of the initial Fourier synthesis and iteratively approximated during the phasing procedure (see below).

Background scatter was eliminated from the deconvoluted intensity profile f(s) by plotting a smooth monotonically decreasing curve through the minima of that profile. The absolute value of the

scattering pattern was then calculated as the square root of these deconvoluted and background-subtracted intensities.

h. Phase analysis

The diffraction patterns from native T7 phage were phased with alternating signs for each maximum (Guinier and Fournet, 1955), again assuming that the structure approximated a sphere of uniform electron density; this assumption was immediately tested by comparing the results of the Fourier synthesis with a spherical model.

For the shell-like structures, there is potential for ambiguity in the interpretation of the signs of the maxima. Because the transform of a shell is the transform of a solid sphere defining the inner shell radius subtracted from the transform of a solid sphere defining the outer shell radius, it is possible for outer orders of diffraction to cancel each other such that the intensity of a peak might drop below noise level. In this case (which can easily be produced with model transforms), while the signs of all successive maxima may alternate, the signs for all observed maxima would not necessarily alternate. Thus, correct phasing for capsids was established by comparison of F(s) with the transforms of model shell structures. A table of Fourier transforms of shells of varying sizes and ratios of inner to outer radii was calculated. In the case of each of the capsids examined, the experimental positions of maxima and minima were compared with the positions of the maxima and minima of transforms in the table, and the signs chosen for each particular structure were those from the ideal transform whose maxima and minima matched most closely. In this manner, the phased

structure factor profile was obtained. (Coincidentally, phases determined by model comparisons did alternate at successive nodes in transforms of the intermediates, although this was not assumed.) Finally a Fourier transform was carried out using

$$\rho(r) = \frac{2}{r} \int_{S=0}^{S} F(s) \sin(2\pi rs)s \, ds$$

to give the radial electron density distribution $\rho(r)$.

i. Estimation of errors in radial parameters

In any radial electron density function $\rho(r)$ which represents a change in electron density at a characteristic radius, the measured change in electron density will be smoothed out by two factors. The first contributor is the fact that the electron density variation in the particle is not a step function, due for example to irregularities in protein surface. The second is that the change in $\rho(r)$ will be broadened due to the resolution limit of the data, in a predictable fashion. In reporting characteristic radii, we refer to the radius at half the peak height in $\rho(r)$. These radii can be measured much more accurately than $\pm s_{max}^{-1}$, where s_{max}^{-1} is the resolution limit. The reason for this is that there is a high correlation (i) between the radius of the shell center and positions of nodes in the transform, and (ii) between the shell thickness and the relative intensities in the data.

An attempt was made to assess the accuracy of such radii by comparing the diffraction from a simple shell structure, capsid IIb (see Figure 1), with diffraction calculated for model shell structures of

different inner and outer radii R_I and R_0. The model structures were step functions of electron density with respect to radius, such that $\rho(r) = 0$ for $0 \leq r < R_I$ and $R_0 < r < \infty$, with $\rho(r) = 1$ for $R_I < r < R_0$. The transform of each model shell, $F_c(s)$, was scaled to the observed data $F_o(s)$ by least squares minimization of the function $\Delta = \int_{s=s_1}^{s_2} (F_o(s) - kF_c(s))ds$ with respect to k, and between the limits s_1 and s_2. The interval s_1 to s_2 was chosen to include all observed data except the zero and first maximum of the transform, where the possibility for data errors is greatest.

The final index of agreement between the model transform and the observed transform was calculated according to

$$R = \frac{\int_{s=s_1}^{s_2} (F_o(s) - kF_c(s))\, ds}{\int_{s=s_1}^{s_2} F_o(s)\, ds} .$$

For capsid IIb, for example, this residual has a minimum value of 19.2% when $R_I = 263$ Å, $R_o = 283$ Å (see below). This figure represents errors due to (i) the difference between the model shell step function and the true radial density function $\rho_T(r)$, (ii) errors in the data, due to measurement and possibly due to interparticle interference.

To assess the contributions of errors due to (ii) above, the data were smoothed by eliminating all components of frequency greater than 500 per $Å^{-1}$ (or wavelength less than $1/500$ $Å^{-1}$). (This was achieved

by Fourier transforming the observed data, $|F_o(s)|$, and back transforming only the component for $0 \leq r < 500$ Å). The residual between the model shell and the smoothed data was 12.3%, while the residual calculated between the smoothed and unsmoothed data was 13.1%. These residuals indicate that random errors due to data recording or to interparticle interference between one virus shell and others in the solution can account for at least 13% of the overall error residual alone (type ii errors). The difference between electron density functions corresponding to the transforms of $F_o(s)$ and $F_c(s)$ was about 10.5% (see Figure 4), indicating that the major part of the minimum residual R = 12.3% is due to (only slight) inadequacy of the step function model as representing the true radial density function $\rho_T(r)$ (type i errors).

In view of the strong coupling between optimal shell center position and optimal shell thickness, the residual was calculated for an array of values R_I, R_O around the optimal radii for capsid IIb, 263 Å and 283 Å, respectively. It was found that a 1 Å change (+/-) in R_I or in R_O, or in both R_I and R_O accounted for at least a 1% increase in the residual. The residual was a smoothly increasing function around the optimal radii; thus we conclude that the accuracy in R_I,R_O values is about ±1 Å, using data to a resolution of 30 Å, and this is an estimate of the errors in radii quoted in Table I.

4. Results

The phased structure factor profiles for each of the species examined are shown in Figure 4. In all but two cases it was possible to follow the spherical diffraction beyond a resolution of 40 Å before

the diffraction dropped below film noise level or the appearance of diffraction due to nonspherical terms rendered the unambiguous assignment of phases impossible. The lowest resolution profile extended to 47 Å (for capsid I-unfixed), corresponding to eleven observed orders of diffraction, and the highest resolution profile (capsid IIb) was unobserved beyond 30 Å and included seventeen orders of diffraction.

The radial electron density profiles resulting from Fourier inversion of the phased structure factor profiles may be seen in Figure 6. The portion of each profile inside that radius equal to the resolution limit of the data is omitted because Fourier series termination errors render it meaningless. A tabulation of significant distances deriving from these profiles is provided in Table I.

a. T7 phage

When phage T7 is prepared for electron microscopy under conditions that do not cause phage flattening, the phage appears to be either a sphere or a polyhedron circumscribed around a sphere, with a short tail (Fraser and Willimas, 1953; Serwer, 1977; Figure 8a). The radial electron density profile $\rho(r)$ for T7 phage is roughly constant out to the edge of the phage, suggesting that the hydrated, packaged DNA has roughly the same electron density as the protein shell of T7 phage. Assuming an anhydrous specific volume for T7 DNA and protein of .55 and .75 ml/gm, respectively, and a hydration of .3 gm/gm for T7 protein (Serwer, 1975), a hydration of 1.42 gm H_2O/gm of DNA is calculated for packaged T7 DNA.

$\rho(r)$ at the phage periphery appears to have a shoulder which contributes about 5 Å to the apparent radius of the phage. We presume

this shoulder to arise from the phage tail. The radius of T7 phage, excluding its tail, was determined to be 301 ± 2 Å, and its volume calculated to be $11.4 \pm .4 \times 10^{-17}$ ml.

b. T7 capsids with phage-like envelopes

To determine the dimensions of the protein envelope of T7, DNA must be removed from the interior of the phage envelope. There are two categories of capsid with an envelope possessing a phage-like protein composition: 1) Capsids IVa (without a tail) and IVb (which has a tail) are obtained by temperature shock of T7 phage which releases the DNA from the whole phage (see Figures 1,7). 2) Capsids IIa and IIb are obtained from wild-type lysates and contain an internal core structure not present in capsids IVa and IVb. This core disintegrates in capsid II during storage (Serwer, 1976a) and only 15% of the capsid II particles had visible cores at the time diffraction experiments were carried out.

The radial density profiles obtained for capsids IVb, IIa and IIb show that all of these capsids are hollow spherical shells. $\rho(r)$ for capsids IIa and IIb are very similar to each other and have shell thicknesses of 23 Å and 20 Å, respectively, with the same inside radius $R_I = 263 \pm 1$ Å. The outer radii are clearly difrerent from one another although the difference is small (3 Å ± 2 Å).[4] The maximum difference in radius between capsids IIa and IIb consistent with the data is 7 Å or about 2.5%, and this is not enough to account for the 7% difference in sedimentation rate observed in sucrose gradients (Serwer, 1976a). Capsid IIa must be either less massive than capsid IIb, less dense in

sucrose gradients, or both. That the latter may be the case is suggested by the observation that capsid IIa has a lower buoyant density than capsid IIb in a cesium chloride density gradient (Serwer, P., unpublished observation).

c. The internal volume of T7 phage and of the envelope

The average value for the volume occupied by the protein envelope in capsids IIa and IIb is $2.0(\pm.15) \times 10^{-17}$ ml. Serwer (1976) found that the volume occupied by anhydrous envelope protein was $2.2(\pm 0.2) \times 10^{-17}$ ml.[5] Thus the protein of the T7 envelope appears to be very tightly packed, and excludes essentially all water from the shell structure itself.

The peak density for capsid IVb is located at the same radius as for capsids IIa,b, although the shell thickness is considerably greater (30 ± 2 Å) in capsid IVb. This difference may be due to the presence of the tail structure, which projects both inside and outside the shell, and accounts for 15% of the mass of capsid IVb (Serwer, 1976; Figure 6b). Therefore, it seems reasonable that the protein envelope of capsid IVb may be very similar to those of capsids IIa and IIb. Nevertheless, the outer radius of capsid IVb (with the tail) is 5.5% smaller than for whole phage. When DNA is contained in whole phage, the outer radius is larger than for any of the empty shell structures.

If the volume occupied by coat protein plus tail were the same in whole phage (outer radius 306 Å) as in capsid IVb (outer radius 289 Å), the inner radius of the T7 envelope would be 280 Å and would enclose a volume of 9.2×10^{-17} ml. Subtracting from this the estimated volume of the hydrated cylindrical core, 0.56×10^{-17} ml (Serwer, 1976), the

volume available to DNA would be 8.6×10^{-17} ml. This is 2.1 times the estimated volume for hydrated T7 DNA in the B form, calculated using the molecular weight of 25.5×10^{6} daltons (Friefelder, 1970), assuming an average molecular weight per base pair of 662 daltons, and that the DNA is represented as a cylinder 10 Å in radius, with one base pair each 3.4 Å.

We have confirmed the 24 Å spacing observed in T7 phage by North and Rich (1961), which they attributed to DNA-DNA spacing. If one assumes that packaged segments of T7 DNA are arranged in a uniform hexagonal lattice with this interplanar spacing, the whole DNA would occupy a volume of 8.7×10^{-17} ml, which is almost exactly equal to the predicted available volume for DNA in T7 (8.6×10^{-17} ml).

d. Capsid I - the prohead of T7

Capsid I is the normal precursor to T7 phage. During the course of DNA packaging two protein components (P9,P19) are lost from capsid I, and the tail structure plus T7 DNA are incorporated. Capsid I particles were prepared both from wild-type T7 lysates and from nonpermissive lysates of the amber mutant 28 which lacks the gene for DNA polymerase. Preparations of capsid I from both sources have similar protein composition, and similar appearance in electron micrographs (see Figure 8) which suggests that there is little difference between particles from both sources (Serwer, unpublished).

Electron microscopy of capsid I particles after centrifugation, however, showed that approximately 90% of the structures had disintegrated during preparation, leaving a large residue of debris on the

grids. Cross linking of particles, by fixing in glutaraldehyde before centrifugation restored the homogeneity of the sample, whereas fixing in glutaraldehyde after centrifugation had no effect. This suggests that the particles are disrupted during the centrifugation step. Thus samples for X-ray diffraction included unfixed proheads (Figure 6d), proheads that had been fixed in glutaraldehyde prior to centrifugation (Figure 6e), and fixed proheads from polymerase minus mutants (Figure 6f).

Radial density profiles for glutaraldehyde fixed capsids I are shown in Figures 6e,f. The inner radius of the shell is some 55-65 Å smaller than for capsids II or IV, which probably have come into contact with DNA (Serwer, 1976). Thus the internal volume of the prohead is about 3.8×10^{-17} ml (calculated for inner radius of 209 Å), minus the volume of internal proteins associated with the hydrated core plus P9 protein (1.16×10^{-17} ml), i.e., about 2.7×10^{-17} ml. The net volume expansion on going from the prohead to whole phage is 5.9×10^{-17} ml, a factor of 2.2, or about 1.4 times the volume estimated for T7 DNA alone.

In spite of the rather large difference between the inner radius of the fixed proheads (209 Å) and of the other shell structures ($\sim$260 Å), the outer radius is only about 25 Å smaller for fixed capsids I than for capsids II and IV. The volume occupied by the envelope in the capsid I shell is a factor of 2.0 larger than for capsid IIb, and the additional volume in capsid I envelope must contain P9 protein, which is lost on contact of capsid I with DNA. The difference in structure between capsids I and II implies a change in the conformation of the major head

protein, P10, which leads to expansion of the shell.

The radial electron density profile indicates that there is some material at low radius in the capsid I structure, presumably due to the presence of the core assembly, and the profile of the edge of the shell is asymmetric, suggesting that the prohead is not adequately described by a simple shell model (Figures 6e,f).

e. Alteration of capsid I on centrifugation

The radial electron density profile for unfixed wild-type capsid I is shown in Figure 6d. The profile indicates that the unfixed particles have expanded considerably with respect to the fixed material. The inner and outer radii are 46 Å and 42 Å larger, respectively. There is indication of a larger amount of material distributed within the "relaxed" prohead, and this is also apparent in electron micrographs (Figures 8a,c).

Storage of capsid I in Tris/Mg buffer at 4° C prior to centrifugation diminished the amount of debris and restored some degree of stability to the prohead. After 12-14 days storage, debris was no longer present on the grids, and this material was used to record the X-ray pattern from wild-type capsid I.

5. Discussion

The model used to phase X-ray scattering data from T7 phage was a sphere with uniform electron density. For capsids IIa and IIb a uniform density spherical shell was used. There are two possible ways in which the real structures may deviate from our models: 1) The perimeter

of the real structure may not be precisely spherical. The most serious possibility in this regard is that the phage and capsid II perimeters may have in solution some of the angularity they have in electron micrographs. This would result in a slight overestimate in shell thickness but minimal error in the mean radii. Second, the electron densities of the real structures may not be uniform at resolutions better than 0.74×30 Å. For instance, it is possible that there is a gap of less than 22 Å between the DNA packaged in T7 phage and the outer envelope.

It is unlikely that there is a gap between the outer envelope of T7 phage and the phage DNA for the following reasons: 1) the envelope decreases in diameter when DNA is removed from T7 phage, suggesting that DNA is exerting pressure on the envelope and is therefore in contact with the envelope. 2) Deletion of part of the DNA from T7 phage results in an increase in the bound water of hydration of the remaining DNA after it is packaged, suggesting that packaged DNA is incompletely hydrated, and binds water until the hydrated DNA fills the inside of the phage envelope (Serwer, 1975).

The internal volume of the capsid of T7 phage (excluding the internal core) was determined from the low-angle data to be $9.2 \pm .2 \times 10^{-17}$ ml, in agreement with the calculation based on DNA-DNA spacings obtained from high-angle X-ray patterns. This is also in agreement with the value of $9.25 \pm .05 \times 10^{-17}$ ml derived from the preferential solvation of packaged T7 DNA in sodium iothalamate density gradients (Serwer, 1975). The hydration of packaged DNA ($\sim$ 1.4 gm H_2O/gm DNA) is high enough so that the DNA should be in the B form.

The volume of T7 phage determined from electron micrographs of phage prepared by negative and positive staining in uranyl acetate, freeze drying, or thin sectioning of embedded phage is significantly lower[6] than the value of $1.14 \pm .05 \times 10^{-16}$ ml reported here (Williams and Fraser, 1973; Serwer, 1976b). The electron microscope values for T7 phage volumes are all equal within experimental error to the anhydrous volume of the sodium salt of T7 phage ($5.0 \pm .015 \times 10^{-17}$ ml) (Serwer, 1977). This strongly suggests that electron microscope values for virus dimensions in general should not be taken too literally. Differences in size between different structures seen in the electron microscope may also be artifactual and may reflect differential dehydration and, in the case of negative staining, differential flattening (Serwer, 1977). The radius estimated from electron micrographs (Serwer, 1977) for T7 phage is 230 Å ± 16 Å, 23% smaller than that observed in solution.

It has been proposed that the force driving DNA into capsid I is a difference in pressure between the inside and outside of the capsid envelope produced when the envelope of capsid I expands (Serwer, 1975). Two requirements of this hypothesis are: 1) the capsid envelope must be impermeable to water during packaging, except at a hole through which DNA is drawn; and 2) the internal volume of the capsid must increase by at least the volume of the DNA packaged.

Capsid permeability to water has not been rigorously investigated. However, the idea that the T7 envelope is impermeable to water is consistent with the extremely high density of protein found present in the

T7 envelope. It may be that water impermeability of the capsid I envelope is involved in the pelleting-induced expansion of capsid I. If the only water permeable location in capsid I is at the hole through which DNA enters, and if capsid I particles aggregate at the high concentrations produced by pelleting (as suggested by the unpublished electron microscopy of P. Serwer) in a hole-to-hole fashion, the aggregated capsid I particles might form a water impermeable complex. A considerable pressure differential due to an acceleration gradient ($\sim$ 1/10 $\times$ G at speeds normal for our sedimentations) could then develop across the capsid membrane when the speed of the centrifuge changes. Such a pressure differential might induce capsid expansion. The decrease in susceptibility to pelleting-induced expansion during storage of capsid I may reflect a loosening of the lattice in the capsid envelope so that small regions can be damaged, thereby increasing the envelope permeability and sparing the remainder of the envelope from pressure damage.

If one assumes that the capsid envelope never becomes any larger than the envelope of T7 phage during DNA packaging, requirement (2) is just satisfied (Results, Section e). However, additional information concerning requirement (2) has recently been obtained through the isolation from wild-type T7 lysates of an infective T7 phage particle (phage II) whose hydrodynamic properties and electron microscope appearance suggest that the outer envelope of phage II is 29% larger in radius than the envelope of normal T7 phage (Serwer, P. and Watson, R., unpublished results). Phage II, isolated by its low density in cesium

chloride density gradients, spontaneously converts to a particle with the density of normal T7 phage, suggesting that it is an intermediate in phage maturation. The difference in internal volume between phage II and capsid I is at least twice the volume of the B form of T7 DNA. Such hyperexpansion of the capsid envelope during DNA packaging would insure that sufficient increase in the volume of the capsid envelope took place to package all DNA, in spite of possible water leaks. The existence of phage II is compatible with the observation of different radii for capsids whose envelopes have similar protein composition (Table I), an observation which suggests that the subunits in the T7 envelope can be accommodated in spherical shells of different curvatures.

To develop models for the capsid I envelope we have assumed that the correct dimensions for capsid I are those of fixed capsid I. This assumption is based on the observation that fixed capsid I which has been pelleted for X-ray diffraction resembles unfixed unpelleted capsid I in the electron microscope.

The $\rho(r)$ of the envelope of capsid I is asymmetrical so that a model with more than two and probably at least four parameters is necessary to fit the data. All the possibilities have not been systematically explored, but the following considerations suggest a plausible model: the value of the outer dimension for fixed capsid I is 261 Å, 8-10% lower than this dimension for the phage-like capsids. The phage-like envelopes clearly have some flexibility because their outer dimension values are smaller than the radius of T7 phage. Therefore, it is proposed that the outer portion of the capsid I envelope is a phage-like shell of P10 whose thickness relative to capsid II has increased in

inverse proportion to the square of the diameter and is therefore 29 ± 4 Å. If so, there must be a second shell of protein inside of the outer shell, and the inner shell must have a greater thickness than the outer shell. If one assumes that this inner shell consists of P9 and only P9, the amount of matter in the inner shell is 32% the amount in the outer shell. From the electron density profile of capsid I (glutaraldehyde-fixed prohead; Figure 7), there is no apparent boundary between the DNA incorporation protein and the major head protein in the envelope profile (although a shoulder is apparent). This would seem to indicate that if there is some space in the P9 protein matrix it may appear between the P9 molecules, rather than between P9 and the major head protein envelope. Attempts at matching a purely spherically symmetric model with these parameters to the diffraction from capsid I have so far proven fruitless, probably due to the presence of the core material.

Footnotes

1. Any structure which contains a protein envelope related to the envelope which surrounds DNA in T7 phage will be referred to as a capsid. A capsid may have proteins in addition to envelope proteins.
2. Phage T7 proteins which are the product of an identified T7 gene will be designated by P followed by the gene number as determined by Studier (1972).
3. Specimen to film distance was 19.5 cm. The centers of the silica flats were located at distances of 9 and 16 cm from the source. Source to specimen distance was 34 cm.
4. It is not known whether capsid IIa or IIb more accurately represents the envelope of T7 phage. Therefore, the average shell center and thickness for these two capsids will be used in future calculations, with an appropriate increase in estimated error.
5. The anhydrous masses of the different components of T7 phage (core, tail, envelope) are determined by determining the fraction of the total proteins in a given component from quantitative densitometry of Coomassie Blue stained SDS gels of T7 phage (Serwer, 1976), and multiplying this by the mass of the entire protein component, 4.05×10^{-17} gm (Bancroft and Freifelder, 1970; Dubin et al., 1970). The anhydrous masses of the internal core, tail and envelope of T7 phage are successively $.54 \times 10^{-17}$ gm, $.42 \times 10^{-17}$ gm, and 3.1×10^{-17} gm. To determine these numbers it was assumed that the core is made of P8, P13, P14, P15, P16; the phage tail consists of

P11, P12, P17; the envelope consists of P10, Q and a small amount of P9 (Serwer, 1976). However, in capsid IVb, P8 associates with the tail (Serwer, 1976).

The anhydrous volume, V_a, of any component is calculated from its anhydrous mass, m_p and its anhydrous specific volume $\bar{V}_p$ using the equation $V_a = m_p \bar{V}_p$. It is assumed that $\bar{V}_p$ is the same as the average $\bar{V}_p$ of T7 phage, .73 ml/gm (Serwer, 1975). The hydrated volume of a component V_h, is calculated from the equation $V_h = m_p(\bar{V}_p + \Gamma)$ where Γ, the hydration, is taken to be .3 gm H_2O/gm (Serwer, 1975). These calculations will be made as needed in the text.

6. It is not yet known whether the decrease in volume occurs during specimen preparation, during exposure to the electron beam, or both.

Acknowledgments

This work was carried out with the support of the National Institutes of Health (grant numbers GM-19984 and GM-70469 to R.M.S.), the National Science Foundation (grant number BMS 75-04105 to R.M.S.), and the U.S. Public Health Service (grant number AI02938 to Dr. W. P. Wood), whose help is gratefully acknowledged. One of us (R.M.S.) is the recipient of a National Institutes of Health career development award, and another (P.S.) received an American Cancer Society postdoctoral fellowship. Two others (J.E.R. and M.J.R.) were supported by National Institutes of Health predoctoral traineeships. This is contribution No. 5610 from the Norman W. Church Laboratory of Chemical Biology, California Institute of Technology.

References

Bancroft, F. C. & Freifelder, D. (1970). J. Mol. Biol. 54, 539-546.

Bragg, W. & Perutz, M. (1952). Proc. Phys. Soc. A 213, 425-435.

Bragg, W. & Perutz, M. (1954). Proc. Phys. Soc. A 225, 264-286.

Casjens, S. & King, J. (1975). Ann. Rev. Biochem. 44, 555-611.

Dubin, S. B., Benadek, G. B., Bancroft, F. S. & Freifelder, D. (1973). J. Mol. Biol. 54, 547-550.

Finch, J. T. & Holmes, K. C. (1967). in Methods in Virology (Marmarosh, K. & Koporowski, H., eds), vol. 3, pp. 351-474, Academic Press, N.J.

Fraser, D. & Williams, R. C. (1953). J. Bact. 65, 167-183.

Gray, H. B. & Hearst, J. E. (1968). J. Mol. Biol. 35, 111-129.

Guinier, A. & Fournet, G. (1955). Small Angle Scattering of X-Rays, Chapter 2, Wiley & Sons, New York.

Harrison, S. H. (1969). J. Mol. Biol. 42, 457-483.

Kellenberger, E. & Sechaud, J. (1957). Virology 3, 256-274.

Lowry, O. H., Rosebrough, N. J., Farr, A. L., & Randall, R. J. (1951). J. Biol. Chem. 193, 265-274.

Mencik, Z. (1974). J. Appl. Cryst. 7, 44-56.

North, A.C.T. & Rich, A. (1961). Nature 191, 1243-1245.

Ross, M. J. & Stroud, R. M. (1977). Acta Cryst. 433, 500-508.

Serwer, P. (1975). J. Mol. Biol. 92, 433-448.

Serwer, P. (1976). J. Mol. Biol.

Serwer, P. (1977). Submitted to J. Ultrastruc. Res.

Stokes, A. R. (1948). Proc. Phys. Soc. A 61, 383-391.

Studier, F. W. (1969). Virology 39, 562-574.

Studier, F. W. (1972). Science 176, 367-376.

Tikchonenko, T. I. (1969). Adv. in Virus Res. 15, 201-290.

Tikchonenko, T. I. (1975). in Comprehensive Virology (Fraenkel-Conrat H. & Wagner, R. R., eds), vol. 5, p. 1, Plenum Press, New York.

Table I

Characteristic radii for T7 phage and capsids

Species	Shell Radii (Å)††		Peak†	Orders	Resolution (Å)
	Outer (R_O)	Inner (R_I)			
Native T7	306			14	39.7
Capsid I (unfixed)	292	255	274	11	47.0
Capsid I (fixed)	261	209	247	12	38.7
Capsid IIa	286	263	275	14	36.8
Capsid IIb	283	263	273	17	30.0
Polymerase minus Capsid I (fixed)	262	209	243	16	35.0
Capsid IVb	289	259	274	12	41.1

†Radius of peak electron density

††Errors in radii R_O, R_I are estimated to be ±1 Å (see text).

Figure Legends

Fig. 1. Phage T7 capsids. The phage T7 capsids to be analyzed are shown in schematic form. Transformations from one type of capsid to another which occur inside of the phage-infected cell are labeled "in vivo". Changes which are induced in the laboratory are labeled with the treatment which produced the change (Serwer (1976) and Experimental Section). The presence of a core, tail or large quantities of P9 is indicated.

Fig. 2. Diffraction patterns for T7 capsid IIb. Pattern on right represents a 77-hour exposure of a 50% solution of capsid IIb. Pattern on the left is recorded from an eleven-hour exposure of the same solution.

Fig. 3. Effect of deconvolution procedure. Beam profile is g(t), observed data profile is h(x), and final result of deconvolution procedure is f(x).

Fig. 4. Comparison of absolute structure factor profiles for capsid IIb (curve B) and for a perfect shell of inner and outer radii at 263 and 283 Å, respectively (curve A). The baseline is raised for A to simplify comparison.

Fig. 5. Phased structure factor profiles. Key: A) T7 phage; B) capsid IIb (inset, capsid IIa, outer orders); C) capsid IVb; D) capsid I (unfixed); E) capsid I (glutaraldehyde-fixed); F) DNA-polymerase minus capsid I (glutaraldehyde-fixed). It should be noted that no smoothing of the data has been performed

in that Fourier components due to film noise do not overlap with the regions of the transform in real space which are of interest.

Fig. 6. Radial electron density profiles. Key: A) T7 phage; B) capsid IIb; C) capsid IVb; D) capsid I (unfixed); E) capsid I (fixed); F) polymerase-minus capsid I (fixed). These profiles are generated by a spherical Fourier transform (see text) of the structure factor profiles shown in Fig. 5. For the purposes of this plot, an exponential cutoff of the form $F' = F\, e^{-s^2 * C}$ has been employed to minimize Fourier cutoff ripples. The value chosen for C resulted in a diminution of at most 30% of the intensity of the outermost maximum with respect to the central maximum. No cutoff was employed to arrive at distances reported in Table I.

Fig. 7. Electron microscopy of T7 phage and capsids. (a) T7 phage, (b) capsid IVb, (c) capsid IIa, (d) capsid I (from a nonpermissive lysate of amber mutant 28).

Fig. 8. Pelleting-induced alteration of capsid I. All samples have been pelleted at 30K RPM for 76 hr in an SW51 rotor.

(a) unfixed, wild-type capsid I (P9 has been released);

(b) fixed, wild-type capsid I;

(c) unfixed, wild-type capsid I (P9 is still present in capsid nearest center of plate);

(d) fixed, mutant capsid I.

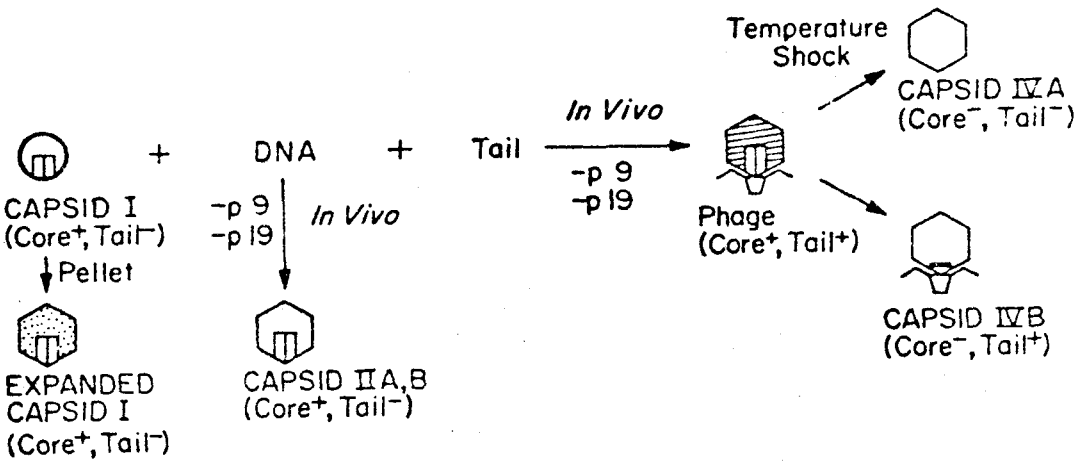
CAPSID I
(Core+, Tail−)
+
DNA
+
Tail
In Vivo
−p 9
−p 19
Pellet
EXPANDED
CAPSID I
(Core+, Tail−)
−p 9
−p 19
In Vivo
CAPSID IIA,B
(Core+, Tail−)
Phage
(Core+, Tail+)
Temperature
Shock
CAPSID IVA
(Core−, Tail−)
CAPSID IVB
(Core−, Tail+)

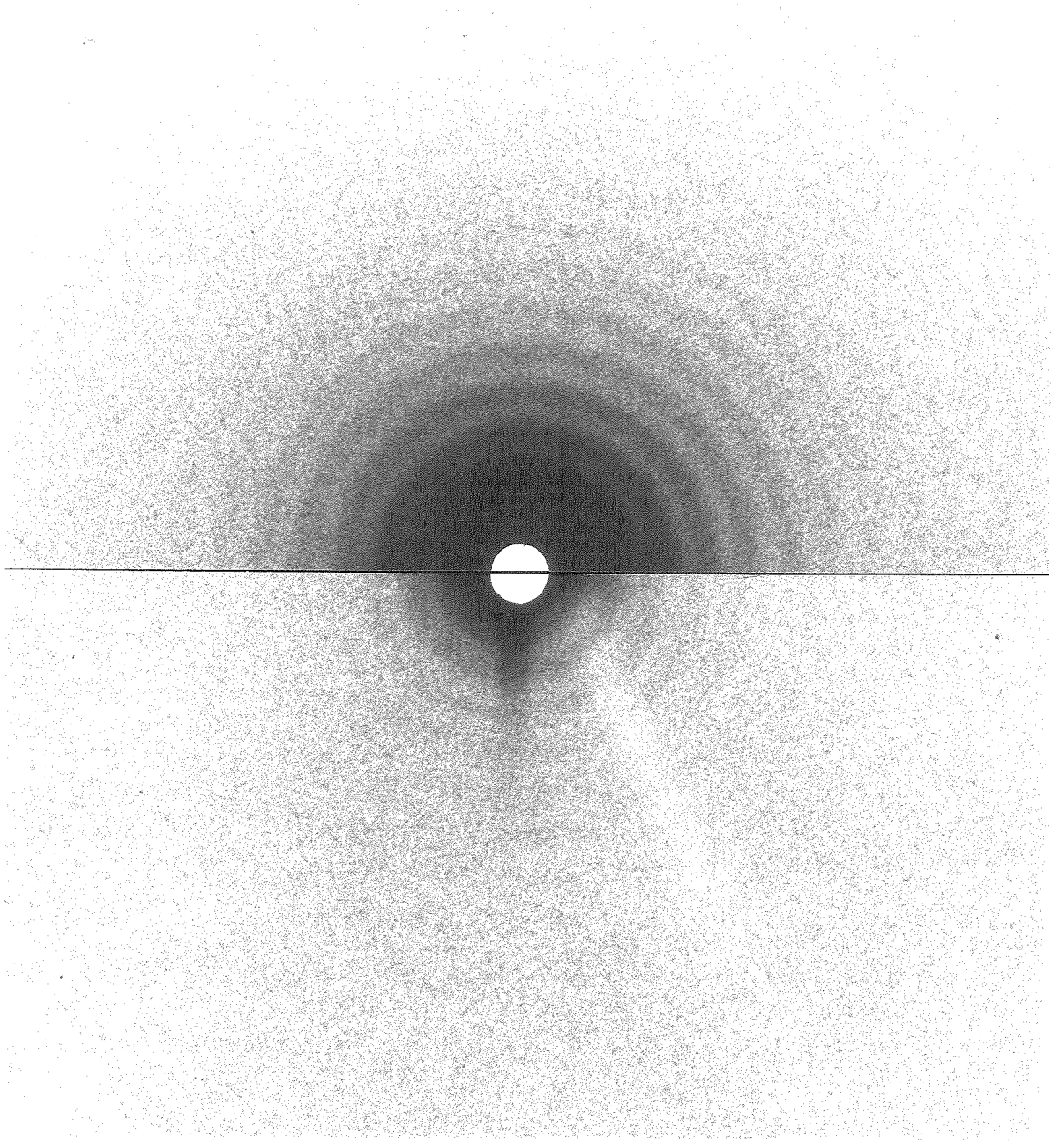

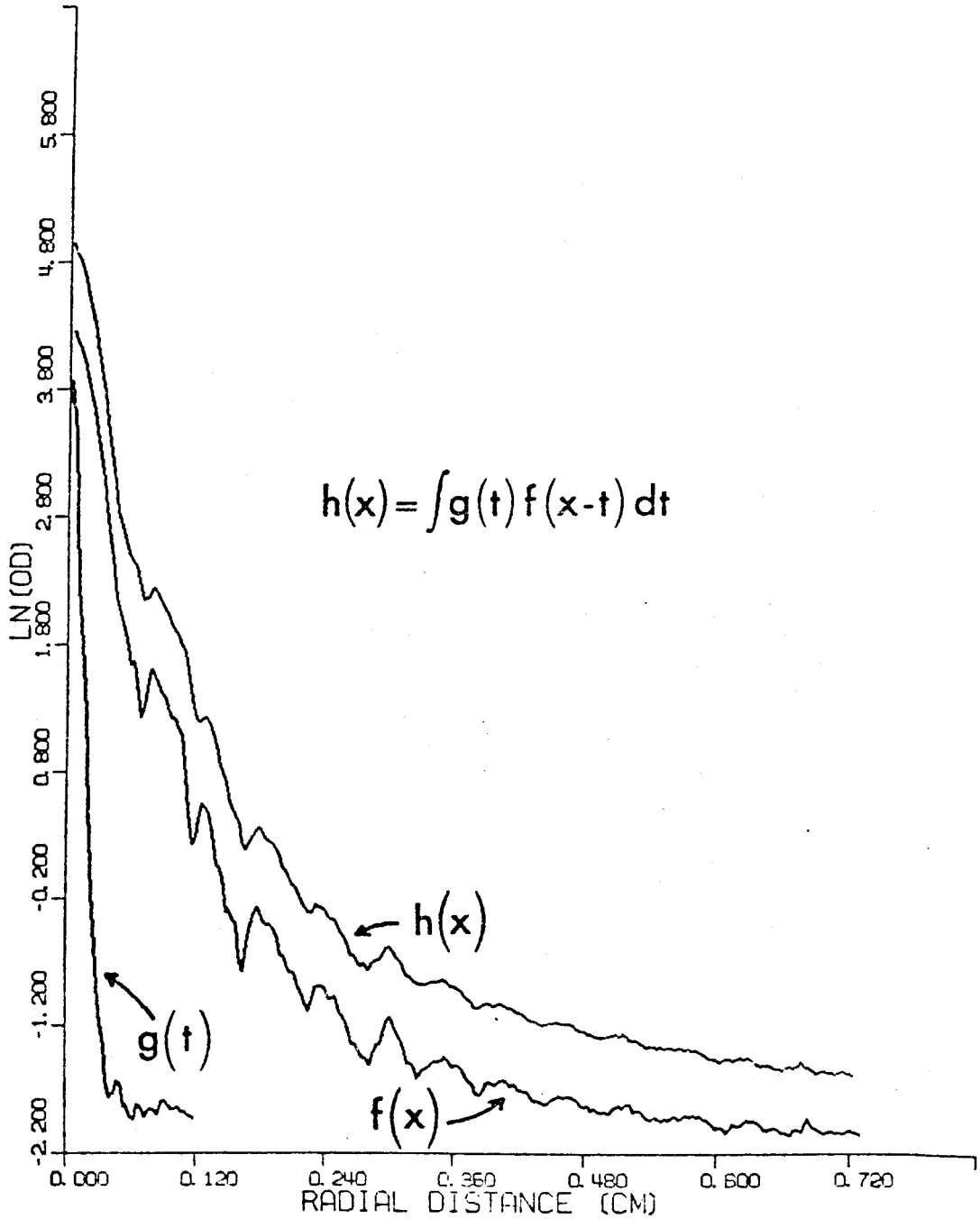
$h(x) = \int g(t) f(x-t)\, dt$
LN(OD)
5.800
4.800
3.800
2.800
1.800
0.800
-0.200
-1.200
-2.200
0.000
0.120
0.240
0.360
0.480
0.600
0.720
RADIAL DISTANCE (CM)
h(x)
g(t)
f(x)

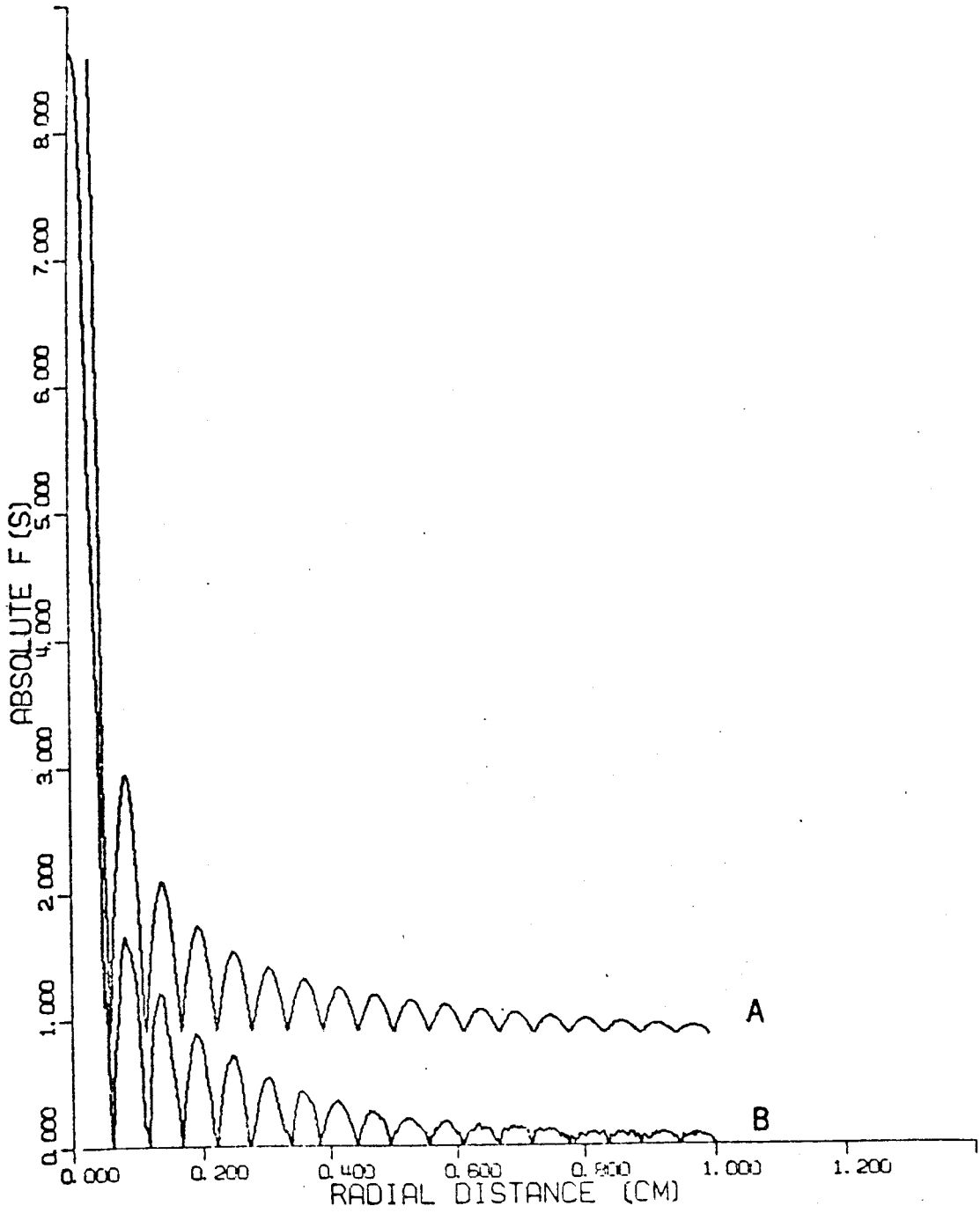
ABSOLUTE F(S)
0.000
1.000
2.000
3.000
4.000
5.000
6.000
7.000
8.000
0.000
0.200
0.400
0.600
0.800
1.000
1.200
RADIAL DISTANCE (CM)
A
B

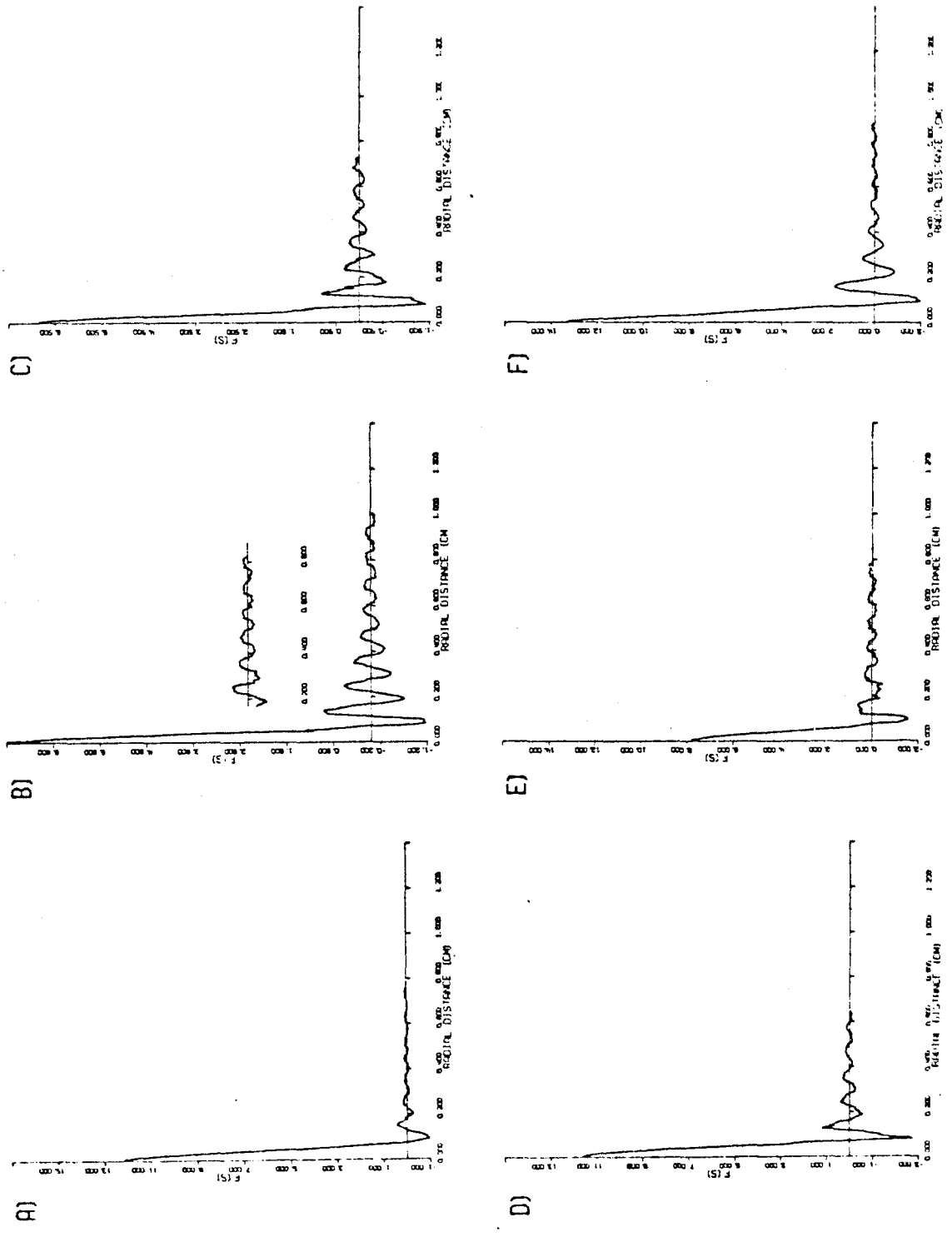
A)
B)
C)
D)
E)
F)
RADIAL DISTANCE (CM)

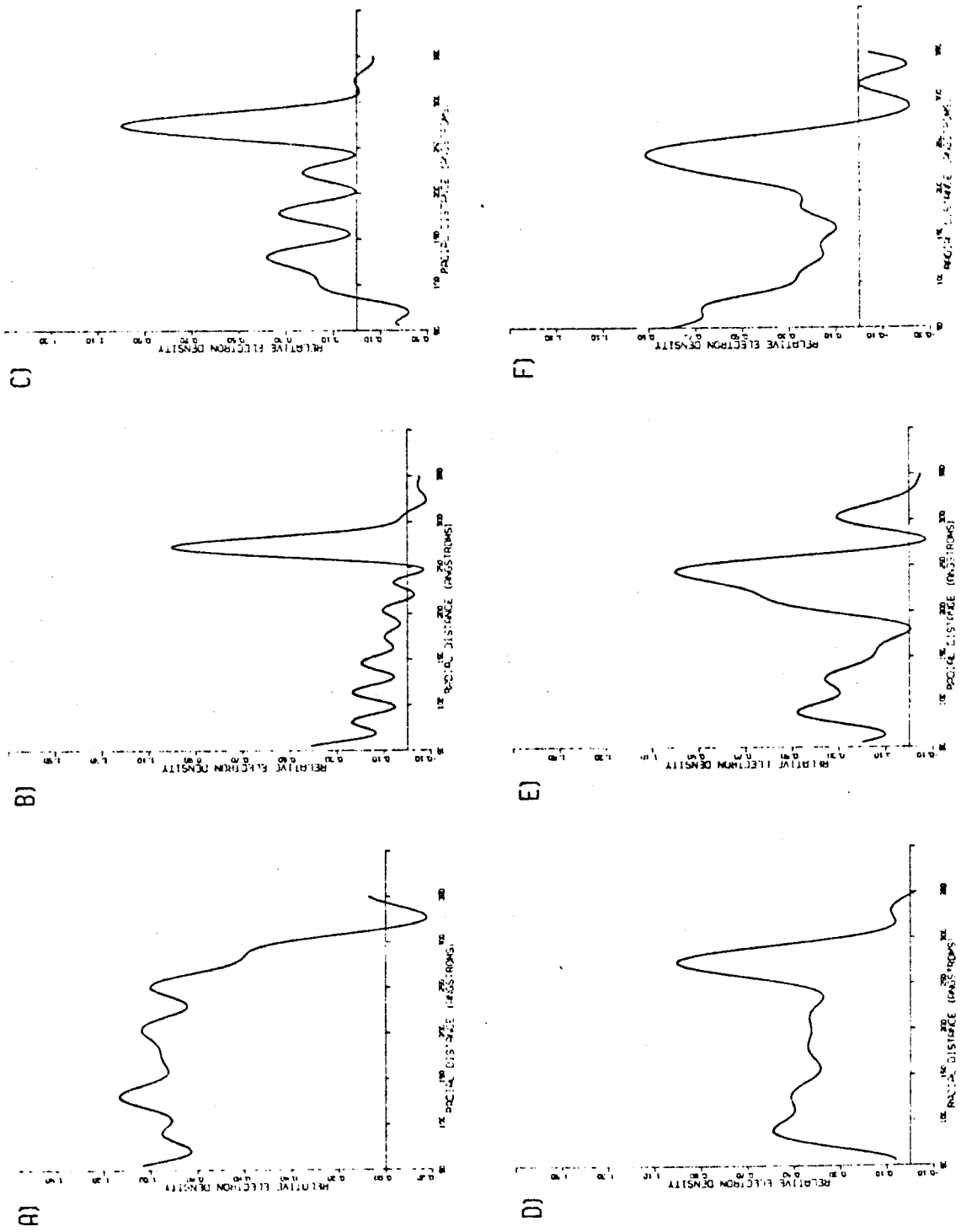
A)
B)
C)
D)
E)
F)

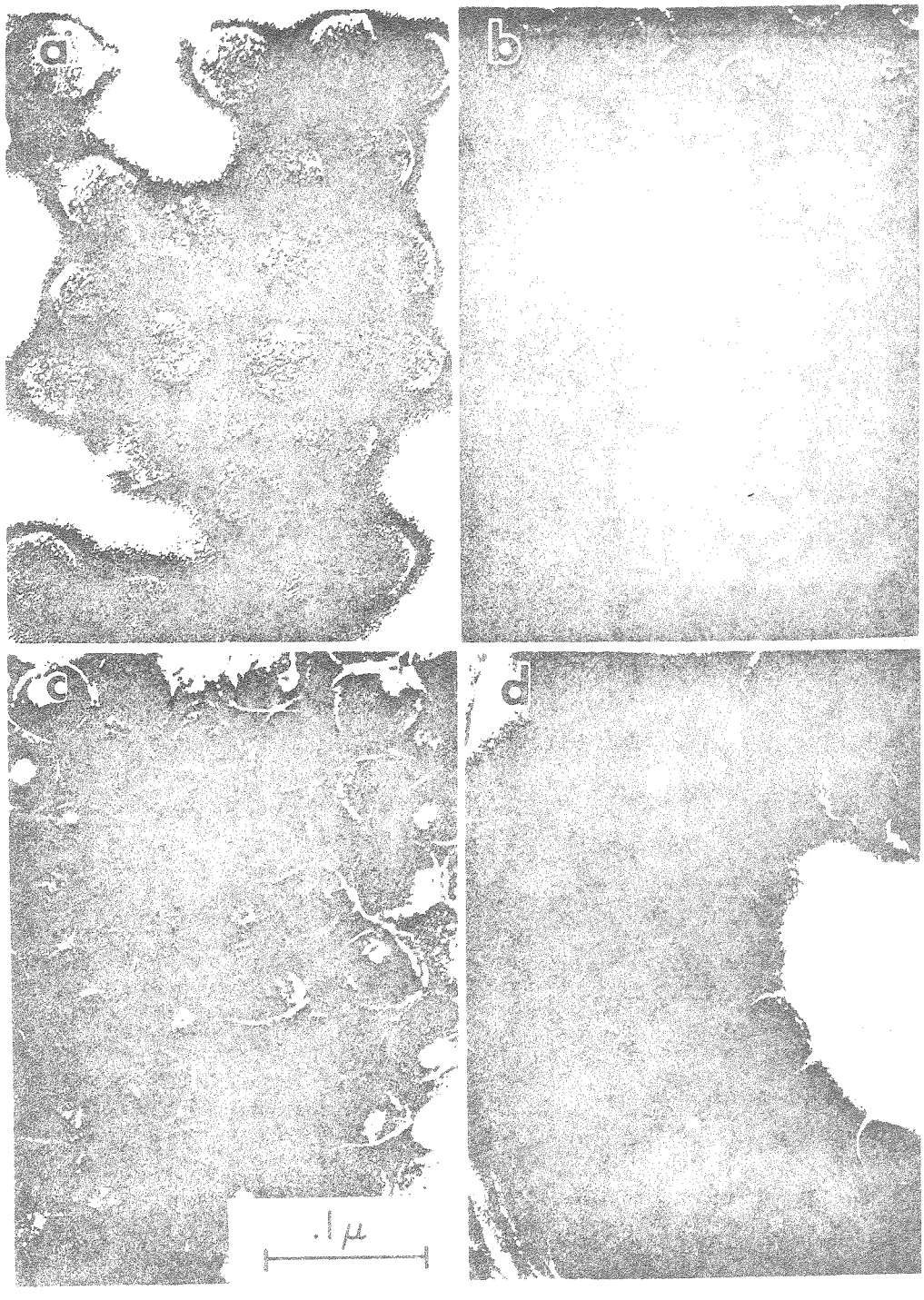
a
b
c
d
.1μ

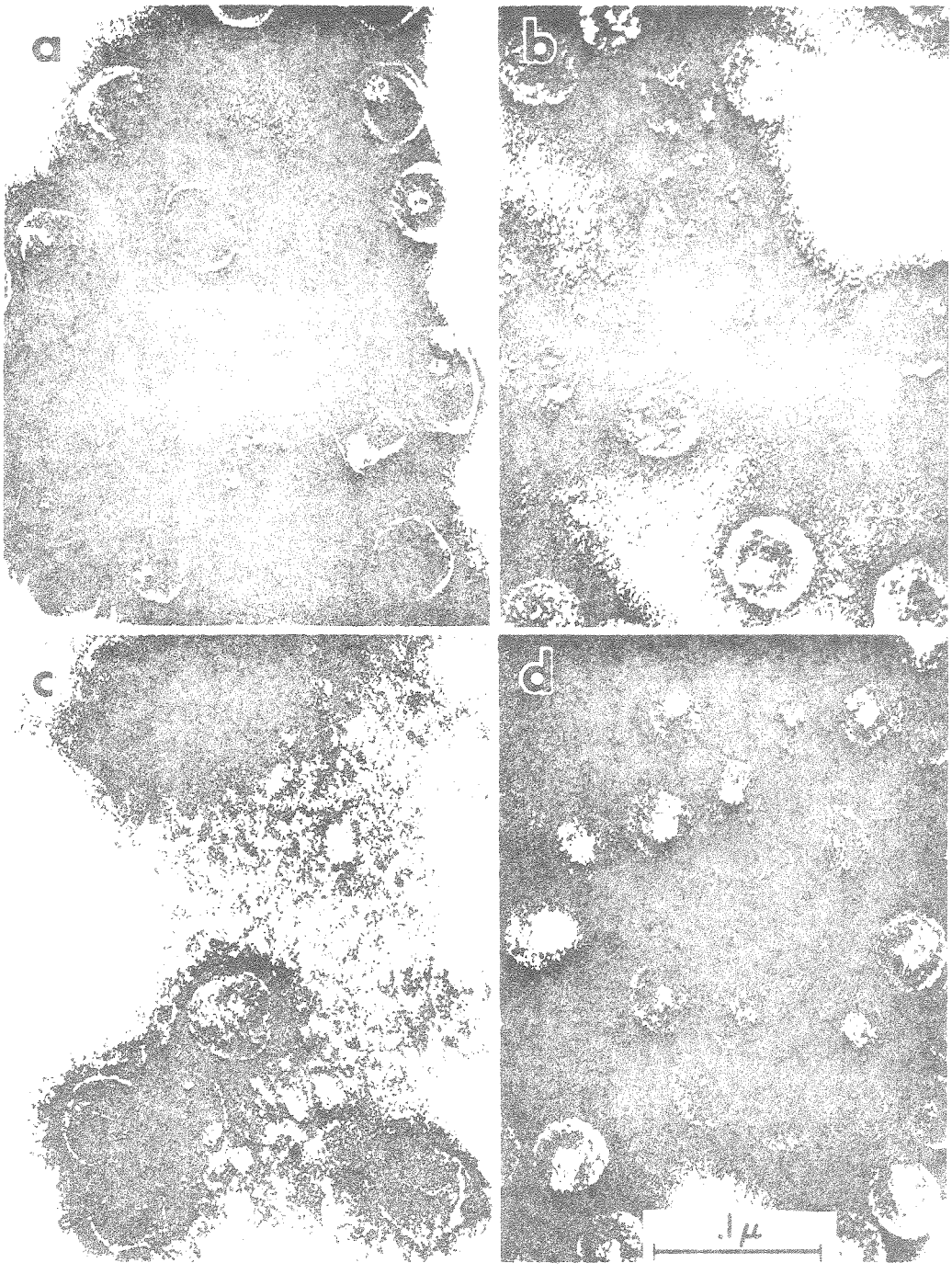
a
b
c
d
.1μ

Appendix B : 'Coda'

Along the bright and thought-infested halls,
throughout the thin and brittle hours of night,
a heady, searing unity is sought;
the sparse, ascetic spirit fast enthralls
the denizens, and breeds a fell delight
in fervent, fretful wars discreetly fought.

So does the stringent deity arise
to wreak its arctic will upon the world;
well-schooled ecclesiastics soon emerge
to focus their fanatic, fevered eyes
upon an austere standard, now unfurled
to drive them to their struggle's icy surge.

Behind the ivory bastions seek the source,
for there, beneath the vast, imposing pile
lie hoards of harsh provender; in the deep
recesses dwell the corpuscles which course
along the glistening arteries, all the while
bound with rigidity immune to sleep.

And all who issue forth, both those who flee
the grim, pervasive grip upon their souls,
and those who grant it welcome, bear a mark --
a deep denial of humanity
with all which can't be counted, or consoles
those sides of man not simple, safe, or stark.

For when the wizened walls at last collapse
in crumbled heaps upon enduring earth,
their missing elements shall stand revealed;
and those who would rebuild them will perhaps
bring <u>all</u> aspects of life to their rebirth,
that ancient illness may be soothed and healed.